Rhythmogram-based analysis for continuous electrographic data of the human brain

Andreas A. Ioannides and Armen Sargsyan

***Abstract*— Ecologically relevant stimuli are rarely used in scientific studies because they are difficult to control. Instead researchers employ simple stimuli with sharp boundaries (in space and time). Here we explore how the rhythmogram can be used to provide the much needed rigorous control of natural continuous stimuli like music and speech. The analysis correlates important features in the timecourse of stimuli with corresponding features in brain activations elicited by the same stimuli. Correlating the identified regularities of the stimulus time course with the features extracted from the activations of each voxel of a tomographic analysis of brain activity provides a powerful view of how different brain regions are influenced by the stimulus at different times and over different (user-selected) timescales. The application of the analysis to tomographic solutions extracted from Magnetoencephalographic (MEG) data recorded while subjects listen to music reveal a surprising and aesthetically pleasing aspect of brain function: an area believed to be specialized for visual processing is recruited to analyze the music after the acoustic signal is transformed to a feature map. The methodology is ideal for exploring processing of complex stimuli, e.g. linguistic structure and meaning and how it fails, for example in developmental dyslexia.**

***Index Terms*— Rhythmogram, Beat spectrum, Continuous data analysis, Dyslexia.**

I. Introduction

THE ambient environment and the activity in the brain share a continuous nature characterized by regularities and unpredictability. Both systems maintain in their ongoing manifestation and activity a memory of the past shaped by fairly stable structures and subtle regularities of their immediate history across different temporal scales. Yet, we study the brain with unnatural simple stimuli that can be repeatedly and identically applied, trapped by earlier successes in natural sciences where rigid mechanical systems were studied. The tendency to use simple artificial stimuli is understandable since they apparently provide the necessary control of unwanted variation allowing the experimenter to study how changes in one stimulus parameter influence brain activity. The conceptual difficulties of this approach are by now well understood but they are tolerated because the reductionist approach has produced a wealth of new and detailed understanding about the brain. Nevertheless, this approach may be too narrow to allow a comprehensive understanding of how the brain functions [1]. There is a theoretical need to augment our understanding of brain function with new knowledge that draws from experiments with ecologically relevant stimuli.

Our earlier attempts to move away from artificial stimuli have used magnetoencephalography (MEG) and specifically tomographic analysis of the MEG signals [2]. We have used auditory stimuli because they are ideal for MEG and because rhythm and regularities in time provide a happy medium between simple stimuli (tones) and environmental sounds. In our first study we emphasized the expectation imposed by a sequence of sounds and demonstrated that silence at the time a tone is expected can create a similar response in the auditory cortex to the response the sound itself would have evoked [3]. In the second example we used the rhythmogram to study how regularities in the music score of authentic music and sound properties (including small changes representing how the performer expressed the music) are reflected in the activity of (different areas of) the brain [4]. The rhythmogram is a two-dimensional self similarity matrix of the signal that is sensitive to subtle regularities in temporal sequences and can be applied equally well to physical signals and to measures of brain activity. We have recently introduced rhythmogram-based analysis to demonstrate that simple and complex rhythms are processed differently in the two hemispheres. However, in [4] we analyzed the response to averaged data. Averaging increases the signal to noise ratio, but may eliminate important details of single trial responses. Here we use a more refined methodology extending the analysis to deal with unaveraged data. We illustrate the power of the basic algorithms with computer generated data, controlling different aspects of noise in the input signal, including the relative strengths of periodic component of interest and non-periodic noise components and the presence of jitter in the single trial responses. We then apply the method to the real tomographic solutions extracted from the single trial MEG signal recorded from musically naïve normal humans.

Manuscript received April 6, 2011. This work was supported in part by the Research Promotion Foundation of Cyprus with upgrade/info/0308/02 and enterprises/product/0609/076 grants.

A.A. Ioannides is with the Laboratory for Human Brain Dynamics, AAISCS (email: a.ioannides@humanbraindynamics.com)

A. Sargsyan is with Neuronal Systems Mathematical Modeling Laboratory, Orbeli Institute of Physiology, Yerevan, Armenia (email: armen_nsmm@yahoo.com)

II. METHODS

We first describe the algorithms for computing the

rhythmogram and beat spectrum of a given signal (Section A), and then present the way we generate the artificial signals used in this study (Section B).

A. Calculation of beat spectrum

The beat spectrum quantifies the signal self-similarity as a function of time lag [5]; peaks correspond to major rhythmic components of the signal, revealing key periodicities across different timescales. The beat spectrum is a robust measure of rhythmic signal constituents with weak, well-characterized dependence on the level of signal noise. The block diagram of the main processing steps for the computation of the rhythmogram and beat spectrum is shown in Fig. 1.

Let $s(t)$ be the signal for which the beat spectrum must be computed, defined by discrete samples at times t_k: $s_k = s(t_k)$, $k = 1, ..., N$. Let $s_w^i(t)$ be the subset of $s(t)$ between $t_i - T/2$ and $t_i + T/2$, i.e. with t_i the center time, and T the size of the window. Computing the beat spectrum of $s(t)$ involves the following three basic steps [4, 5]:

Step 1) Parameterization of the signal. The Fourier transform (FT) $F_i(j2\pi f)$ of $s_w^i(t)$, $i = 1, ..., N_w$, $j = \sqrt{-1}$, is calculated for all time windows (N_w is the number of time windows). The feature vectors are defined as

$$\mathbf{V}_i = \left|F_i(j2\pi f)\right| = \sqrt{\mathrm{Re}(2\pi f)^2 + \mathrm{Im}(2\pi f)^2} \quad (1)$$

(the amplitude frequency characteristic, AFC), where $\mathrm{Re}(2\pi f)$ and $\mathrm{Im}(2\pi f)$ are the real and imaginary frequency characteristics (the cosine and sine Fourier transforms).

An effective algorithm for discrete Fourier transform computation was used that allows to calculate the real and imaginary frequency characteristics for arbitrarily chosen frequencies, i.e., in any frequency range and for any frequency sampling rate.

The result of this step is the spectrogram, i.e. a two-dimensional time-frequency distribution representing frequency specific changes over time.

Any one or combination of the following three optional pre-processing steps may be performed (only the first two were used in the current work):

1) For each window, the signal is centered at zero, by subtracting the window mean, before FT calculation:

$$s_{wc}^i(t_k) = s_w^i(t_k) - \overline{s_w^i}, \quad \overline{s_w^i} = \frac{1}{K}\sum_{k=1}^{K} s_w^i(t_k) \quad (2)$$

where K is the number of samples in the window.

2) The power spectrum is used instead of amplitude frequency characteristic:

$$\mathbf{P}_i = (\mathbf{V}_i)^2 = \mathrm{Re}(2\pi f)^2 + \mathrm{Im}(2\pi f)^2 \quad (3)$$

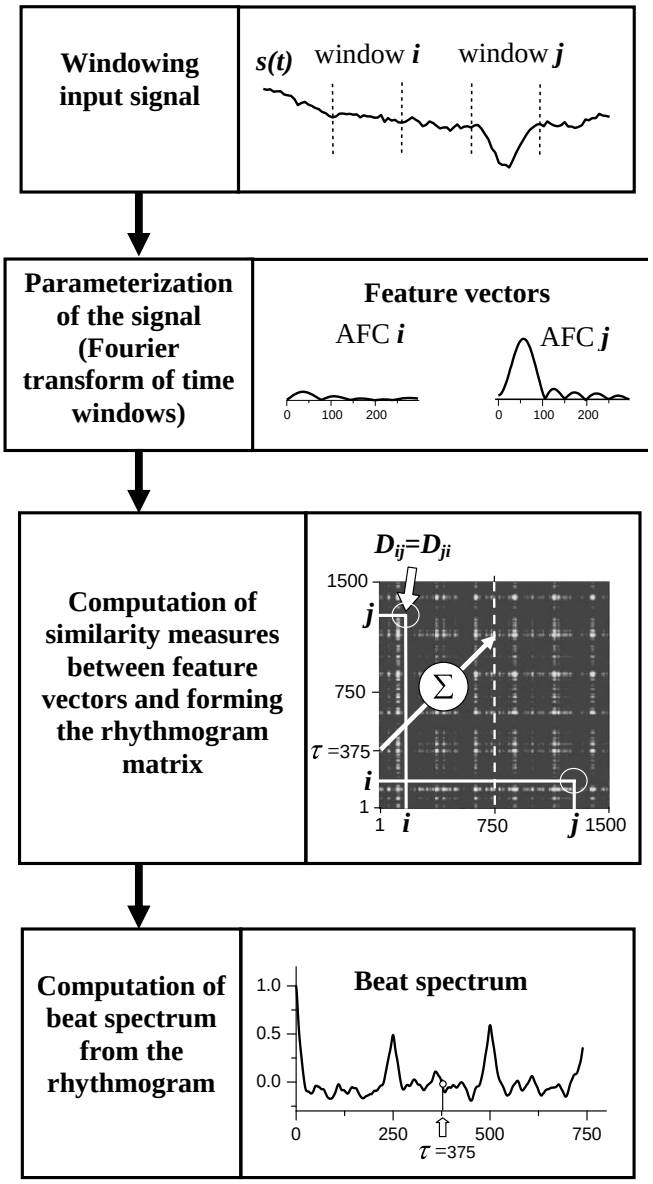

Fig.1. Block diagram of the algorithm for the computation of the beat spectrum. The first block shows the *i* and *j* windows, two arbitrary segments of the input signal *s*(*t*). The second block shows the corresponding AFCs, or feature vectors, one for window *i* and one for window *j*. The third block shows the rhythmogram – two-dimensional matrix formed from integrals of the similarity measures *D* between the feature vectors (AFCs). The values of *D* in the figure are coded in gray scale with dark corresponding to small values and bright – to large values of *D*. The final block shows the corresponding beat spectrum which is an integral across lines parallel to the main diagonal of the rhythmogram and separated from it by a fixed time lag τ. The computation of the beat spectrum point corresponding to a lag τ=375 ms (highlighted by the arrow in the last block) is computed by summing across the line parallel to the main diagonal with the sum sign beginning at the *i*-value corresponding to τ=375 ms.

3) The mean feature vector $\overline{\mathbf{V}}$ is calculated by averaging $\mathbf{V}_i$ ($i = 1, ..., N_w$) and then subtracted from each window's feature vector: $\mathbf{V}_i = \mathbf{V}_i - \overline{\mathbf{V}}$.

Step 2) Computation of similarity measures between feature

vectors (matrices) for successive temporal windows of the spectrograms. The distance measures D_{ij}, $i = 1,...,N_W$, $j = 1,...,N_W$ between all feature vectors $\mathbf{V}_i$ are calculated as a scalar product in the M-dimensional parameter space (where M, the size of $\mathbf{V}_i$, is the number of frequency samples):

$$D_{ij} = \frac{\mathbf{V}_i \cdot \mathbf{V}_j}{A(\|\mathbf{V}_i\|\|\mathbf{V}_j\| - 1) + 1}, \quad (4)$$

where $\mathbf{V}_i$ and $\mathbf{V}_j$ are the feature vectors of i-th and j-th temporal windows. The dependence of D_{ij} on magnitude of $\mathbf{V}_i$ and $\mathbf{V}_j$ is controlled by a parameter A which varies from 0 to 1 allowing continuity from normalized to unnormalized cases. When $A = 1$, D_{ij} is the cosine of angle between vectors $\mathbf{V}_i$ and $\mathbf{V}_j$ When $A = 0$, D_{ij} is the scalar product of $\mathbf{V}_i$ and $\mathbf{V}_j$.

The matrix $\mathbf{D} = (D_{i,j})_{N_B \times N_B}$ is the rhythmogram, from which the beat spectrum is calculated.

Step 3) The periodicity and relative strength of the transient responses are straightforwardly derived from the rhythmogram matrix using the estimate of the "beat spectrum", computed from the autocorrelation of the rhythmogram matrix, as a function of time lag τ:

$$B(\tau_k) = B_k = \sum_{i=1}^{N_B} D_{i,i+k}, \quad k = 1,...,N_B, \; N_B = N_W / 2. \quad (5)$$

Optionally, the beat spectrum may be normalized so that the maximum is always one:

$$B_k^N = B_k / B_{\max}, \quad (6)$$

where $B_{\max} = \max(|B_k|)$, $k = 1,...,N_B$.

The maximum of beat spectrum is always at 0. Thus, any two beat spectra will always correlate well in their initial part. To reduce this undesirable effect, the beat spectrum may be multiplied by the following window function to set its edges to 0:

$$w(t) = (1 - \exp(-t / t_1)) / (1 + \exp((t - t_2) / a)), \quad (7)$$

Here we used the following values: a = 10.0, t_1 = 4 ms, and t_2 0.9 times the maximal time lag of the beat spectrum.

B. B. Generation of the artificial signal

The artificially generated signal is a sum of several components that may be of two types: periodic and random (Fig. 2). The signal may contain arbitrary number of components of each type.

The periodic component is formed by regular repetitions of a finite piece of signal (Fig. 2, A, B). To avoid discontinuities, the transition from the end of the current repeated segment to the next must be smooth. In our case this is achieved simply by having a zero level flat part at the beginning and at the end of the repeated segment.

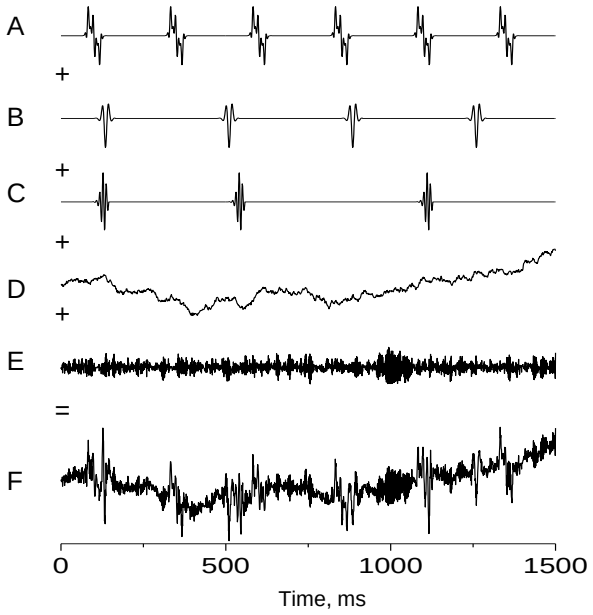

Fig. 2. Illustration of how the artificial signal is generated. In this example, the resulting signal (F) consists of two different periodic components (A and B), one aperiodic component (the periods are randomized) (C) and two different continuous random components (D and E).

The piece represents a sum of arbitrary number of sine waves of different magnitudes, frequencies and phases (which allows obtaining signals with various frequency contents), multiplied by a window function $w(t)$ to smoothly set the edges of the piece to zero (Fig. 3):

$$p(t) = w(t) \sum_{k=1}^{M} a_k \sin(2\pi f_k t + \varphi_k), \quad (8)$$

where

$$w(t) = \frac{1}{1 + \exp(-\alpha(t - \tau_1))} - \frac{1}{1 + \exp(-\alpha(t - \tau_2))}, \quad (9)$$

M is the number of sine waves used, a_k, f_k and φ_k are the magnitude, frequency and phase of k-th sine wave, correspondingly, $w(t)$ is the window function, τ_1 and τ_2 define the width of the window, α defines the slope of the window edges ($\alpha > 0$).

Each periodic component may have different period. This gives a possibility to generate a signal that has two or more different repeating parts that are independent.

Some random fluctuations in the interval between the repetitions of the identical piece of the signal may be introduced (by randomizing, within given limits, the starting point of each repeating identical piece, Fig. 2, C) to study the sensitivity of the method to rhythm irregularities.

The random component (Fig. 2, D, E) is modeled using an

autoregressive process of user-defined order *p*. For each discrete time t_i ($i=1,...,N$) the value of random component $r_i = r(t_i)$ is formed as:

$$r_i = \sum_{k=1}^{p} a_k r_{i-k} + h_i \quad , \tag{10}$$

where h_i is a random number having either Gaussian or uniform distribution with zero mean and given variance *v*, $a_1,...a_p$ are given parameters of the autoregressive model.

The initial value, r_0, may be chosen arbitrarily and provides an initial offset to the signal. In our calculations $r_0 = 0$ was used.

When *p*=0 (zero-order process), then simply $r_i = h_i$. In case of first-order process (*p*=1),

$$r_i = a r_{i-1} + h_i \quad . \tag{11}$$

When $|a|<1$, the first-order process is covariance-stationary (i.e., 1st and 2nd moments do not vary with respect to time). When $a=1$, the process is not covariance-stationary (as in Fig. 2, D).

There may be an arbitrary number of random components, each with different properties.

In the examples we quantified the relative influence of the random component to the artificially generated signal using a simple definition for the signal to noise ratio (SNR), namely the ratio of the periodic to the random component power:

$$SNR = \frac{P_{per}}{P_{rand}} = \left(\frac{A_{per}}{A_{rand}} \right)^2 \quad , \tag{12}$$

where A_{per} and A_{rand} are root mean square amplitudes of periodic and random components, respectively.

III. RESULTS AND DISCUSSION

A. Experiments with artificial data

In the experiments with artificial signals the periodic component of the signal (Fig. 3, left top trace) consisted of six repetitions of the piece shown in inset. The piece was formed by a single sine wave of 50 Hz multiplied by a bell-shape window function. The period was 250 ms and the total duration of the signal was 1500 ms. The random component was generated as earlier described, using an autoregressive model of order one with a_1=1.0 (non-stationary case).

To investigate the dependence of beat spectrum on SNR, the magnitude of the random component was varied while keeping the magnitude of periodic component constant. The resulting signals are shown in Fig. 3, left column. The normalized beat spectra of the signals calculated using 20 ms window size are shown in the right column of Fig. 3.

Since the duration of the signal is 1500 ms, the time lag range we can use for the beat spectrum is 750 ms –half of the signal duration, as follows from the beat spectrum calculation method and inspecting Fig.1. With these parameters, the beat spectrum of the periodic component (Fig. 3, right top trace) has clear peaks at 250, 500 and 750 ms time lags (the latter is not well seen on the figure), which correspond to the period of the repeating piece of the periodic component. For a noise-free signal (no random component) or small noise level, the beat spectrum clearly reveals the repetitions in the signal (peaks at 250 and 500 ms, marked by dotted lines). For large random components the beat spectrum still has peaks at 250 and 500 ms, but they are small and comparable with other "noisy" peaks.

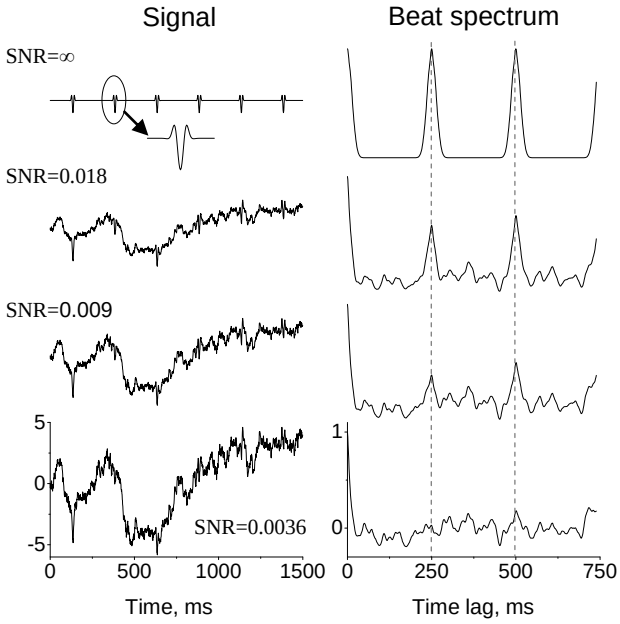

Fig. 3. Dependence of the beat spectrum on the SNR. The random component was generated by a Gaussian pseudo-random number generator routine using the same seed value for all cases, thus the random components for different values of SNR differ only in magnitude. The Y-scale (arbitrary units) is the same for all signal traces. The beat spectra are normalized so they are dimensionless (see Methods).

Next, the dependence of beat spectrum on the size of running time window was investigated. The window size was varied from 10 ms to 40 ms (note that the duration of non-zero part of the periodically repeating signal piece shown in inset in Fig. 3 is about 50 ms and the period of the main frequency component (50 Hz) is 20 ms). In all cases the window was moving along the signal with 1 ms step, which is equal to signal's sampling step. Fig. 4 shows the beat spectra for different window sizes, for SNR=0.018. Small windows produce sharper peaks on the beat spectrum; the reason for this is that large windows, moving with small step, produce more blurred rhythmogram.

In the next series of tests the frequency content of the random component was close to the frequency of the repeating periodic component. This case may mimic more closely the real data, where the signal contains both relevant to stimulus and irrelevant, but similar activations. The periodic component used in this series was the same as in Fig. 3. The random component

was generated using a 4th order autoregressive model with following parameters: a_1=1.0, a_2=0.01, a_3=-0.5, a_4=0.1, the SNR value in this case was 0.128. The first 300 ms of the 1500 ms-long signal and its components are shown in Fig. 5, left column. The signal containing both random and periodic components (Fig. 5, C, left trace) looks very similar to the random component alone (Fig. 5, B, left trace). Although the presence of the periodic component in the signal is visually indistinguishable, on the beat spectrum of the signal (Fig. 5, C, and right trace) there are clear peaks caused by the periodic component (at 250 and 500 ms time lags). These peaks are slightly larger than the peaks caused by the random component and hence technically distinguishable (this was the case also for several other similar signals tested, data not shown). For this figure, the beat spectrum was calculated using the power spectrum (3) (the square of the AFC) of the window signal instead of the AFC, which resulted in slightly more pronounced peaks of interest in the beat spectrum.

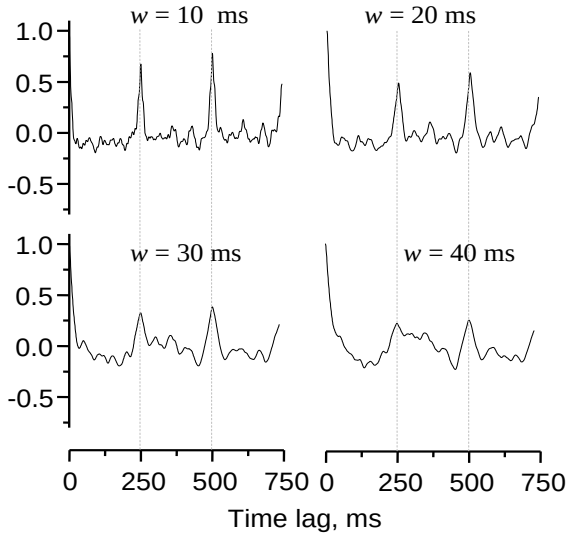

Fig. 4. Dependence of beat spectrum on the size of running time window, *w*.

In real biological responses, events of interest are superimposed with irrelevant events that generate comparable random noise, just as in the above case. Averaging of many repetitions of the response (single trials) will selectively enhance the biological responses to repeating identical external events provided the internal response to each identical external event is precisely reproducible in each single trial. However, if this condition is not held, averaging will eliminate responses of interests together with noise [6]. Real biological systems in general and brain responses to external stimuli in particular are highly variable and this has been one of the main criticisms of averaging for a long time.

The beat spectrum method has an inherent robustness to variations in response onset latency and can therefore provide improvements to averaging single trial evoked responses. The beat spectrum emphasizes the overlap between repeated

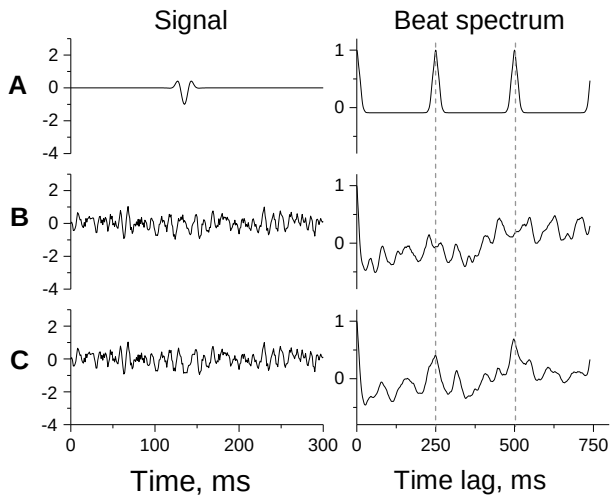

Fig. 5. Example of a signal (C, left column) with random component (B, left column) that has frequency contents similar to that of the periodically repeating piece (A). Right column shows the beat spectra of the periodic and random components (A and B, correspondingly) and the signal itself (C), calculated using the power spectrum.

patterns; if there is some jitter in the onset of the first pattern the peaks in the beat spectrum will be unchanged, provided the latency lag between the repeated patterns is maintained. A jitter in the latency lag between the repeated patterns will simply move the peaks of the beat spectrum. Averaging the beat spectra of different single trials will therefore still produce (broadened) peaks as long as the jitter is not too large compared to the duration of the basic pattern and much smaller than the actual mean lag between repeated patterns. To investigate this expected robustness of the rhythmogram analysis we generated a number of artificial "single trials", where the random and periodic components were produced in the same way (and with the same parameters) as for previous case (Fig. 5), but with the period of the periodic component varying across single trials. The jitter across single trials was restricted to different levels across different tests. The jitter in time, introduced a misalignment of the repeating pieces of periodic component across single trials, and thus limiting the effectiveness of averaging.

For each single trial, the beat spectrum was calculated, and then these single trial beat spectra were averaged. Fig. 6 shows the results for the averaged single trial signals and averaged single trial beat spectra for three different values of period jitter (10, 20 and 50 ms, or 20%, 40% and 100% of the non-zero part of the repeating piece. The left column of the Fig. 6 ("Signal") shows the averages of 10 (upper traces in each plot), 50 (middle traces) and 100 (lower traces) single trials for the jitter values of 10 (row A), 20 (raw B) and 50 (raw C) ms. The right column of the same figure shows the corresponding averaged single trial beat spectra (dotted line – average of 10 single trial beat spectra, dashed line – average of 50, solid line – average of 100). As expected, when the time jitter is small, averaging helps in revealing the periodic component (compare traces of averages in Fig. 6, A, left column, with a single trial shown in Fig. 5, C, left column). Also as expected, as the jitter increases, averaging

become increasingly ineffective, failing to emphasize the periodic component. When the jitter is 50 ms (100%), increasing the number of averaged single trials does not seem to play any role – the periodic component is essentially untraceable in all three traces in Fig. 6, C (left column).

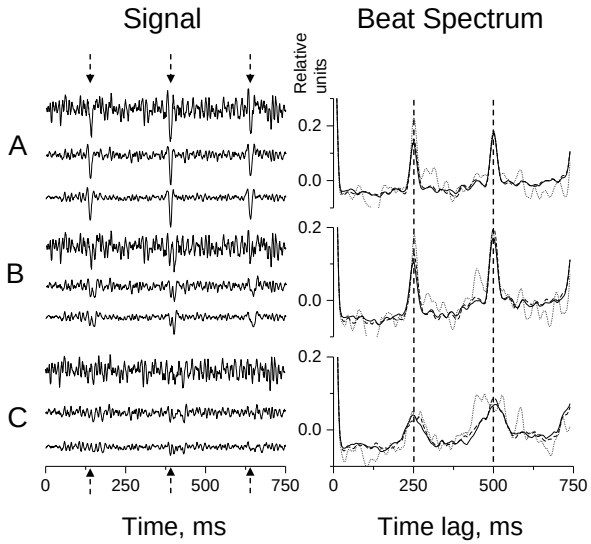

Fig. 6. Results of averaging of the signal and beat spectrum when there is a temporal jitter in the period of the periodic component. A, B, C : jitter of 10, 20, and 50 ms, correspondingly. In the Signal column: upper trace in each plot - average of 10 single trials, middle trace – average of 50 single trials, bottom trace – average of 100 single trials. The arrows show the centers of the repeating piece of the periodic component as if there would be no jitter in time. In the Beat spectrum column: dotted line – average of 10 single trials, dashed line – average of 50 single trials, solid line – average of 100 single trials. Vertical dashed lines show the time lags corresponding to the period of the repeating piece of the periodic component as if there would be no jitter in time.

For the beat spectrum, however, increasing the number of averaged single trial beat spectra improves the quality of the average for all jitter values: the noisy peaks, present on the average of 10 single trials (Fig. 6, right column, dotted lines), disappear as the number of averaged single trial beat spectra increases (dashed and solid lines – 50 and 100 single trials, correspondingly). Even in the case of 100% jitter, the averaged across 50 and 100 single trials beat spectrum shows clear (though wider) and easily distinguishable peaks at 250, 500 and 750 ms time lags.

B. Processing of real MEG data (listening to a musical stimulus)

In our earlier study [4] the musical stimulus (a part of Frantz Liszt's Etudes d'execution transcendante d'apre`s Paganini, S.141-No. 5) of entire duration of 10 s was separated into four segments, for which the beat spectra were calculated and analyzed. The MEG signal from 20 presentations of the piece was averaged and the tomographic solution was extracted for each timeslice of the average data using the CURRY 4.5 source localization software (Philips Res. Lab.). Regions of interest (ROIs) were then defined and treated in exactly the same way as the music score. The correlation of the beat spectra of the music score and from each ROI were the measures representing how well the brain area corresponding to each ROI tracked the music.

There were four major differences between the present and earlier study. First, the tomographic analysis was done using magnetic field tomography (MFT) [7, 8] allowing maximum use of the information in the signals in each timeslice of each single trial [2]. Second, the beat spectrum of the entire motif was calculated. The beat spectrum (Fig. 7, C) computed after the amplitude modulation (AM) component was extracted (Fig. 7, A) reveals the most consistently and rhythmically repeating fragments of the motif – the note triads. Note that the notes themselves are not that periodic, since their duration varies inside each triad (Fig. 7, B).

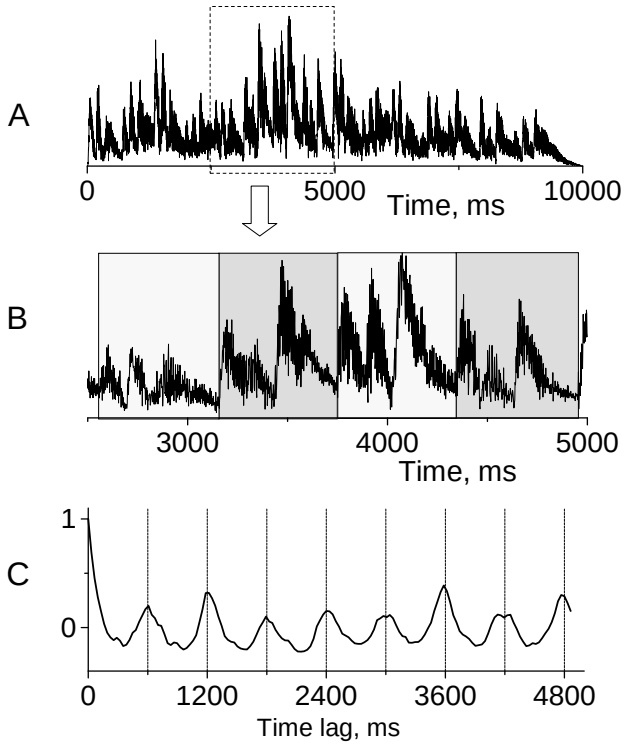

Fig. 7. Beat spectrum of musical stimulus A. The envelope (amplitude modulation) of the music score (the stimulus). B. A fragment of the music score envelope with highlighted consecutive triads of notes. The duration of each triad is approximately 600 ms throughout entire music score (except the very first and two last triads, which are a little longer, about 700 ms). C. The beat spectrum of the entire music score envelope (A) calculated using the window size 200 ms. Vertical lines show that peaks of the beat spectrum appear at time lags that are multiples of 600 ms – the duration of triads in the music score.

The third departure from the earlier study was the single trial tomographic analysis that provided the spatiotemporal changes in activity across the brain for each single trial at millisecond time resolutions. The fourth and final change from the previous study was the computation of the rhythmogram and beat spectra for each voxel (of each single trial) in the brain. The correlation between the beat spectra of the music score and the brain activations from each voxel produces time-dependent tomographic maps describing the brain response to the music score in each single trial and at different timescales (depending on what parameter choices were made for the corresponding

rhythmogram).

One of the key results of the new analysis is displayed in Fig. 8. The figure shows an area in the fusiform gyrus that generates activity with beat spectra sharing the same features as the music score for each of the five subjects studied. The Talairach coordinates (TC) [9] for the centre of this area are: *x*=-25, *y*=-59, *z*=-9. These TC coordinates are remarkably close to the TC for the area reported by many people to be sensitive to face stimuli. To the best of our knowledge this is the first English report of activity close to what has been called the fusiform face area (FFA), in the analysis of music. The result has only been reported before in a Greek essay comparing the neuronal processing involved in the analysis of images and music [10].

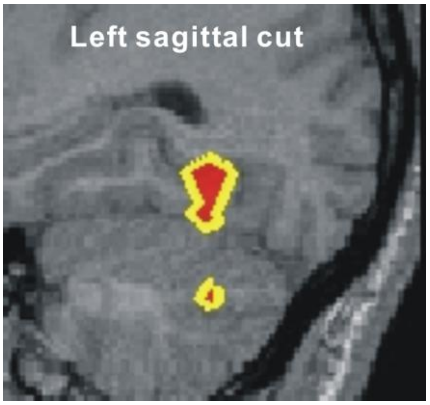

Fig. 8. To obtain this image the overlap between beat spectrum of the music score and the beat spectrum for the activity in each point in the brain was computed, separately for each of five subjects. The results were transformed to a common reference brain and the areas showing statistically significant overlap across all subjects identified. The contours delineate the brain area with common high overlap between the music and brain beat spectra after back transformation to the MRI of one subject, so that the contour is shown together with the background anatomy. In addition to a small region of the cerebellum the main activation is in the fusiform gyrus.

Our results show that when we listen to music, the changes in activity in one of the key brain areas related to processing of complex visual stimuli reflect the repeated patterns in the music score. A mundane explanation of this observation might be that the emphasis in the auditory modality is reflected by an inhibition of activity in this primarily visual area; this explanation however fails to explain why only this specific and highly specialized area behaves in this way. A more parsimonious interpretation will be that the first analysis of the auditory input (in the auditory cortex) produces a frequency map which is then analyzed as a complex pattern by the same area that analyzes complex visual patterns. This line of reasoning would then suggest that a complex and structured auditory stimulus, like music, should in some way be perceived as similar to an image. Why then there is no trace of visual perception when we listen to music? This may be because recent evolutionary pressure put the emphasis on language competence thus deemphasizing visual aspects of perception that music might evoke. What seems to be important for language is the accurate parsing of words to extract their meaning rather than the "shaping" of the linguistic material. Dyslexic children have difficulties with timing, as is evidenced by the correlation between spelling ability and the skill of tapping out the rhythm of a song [11]. Interestingly some dyslexic musicians are forced by their learning difficulties to "focus on music beyond the notes"; they report seeing "partterns and shapes in music" that others do not perceive [12]. Rhythm skills and learning skills requiring rapid processing of novel stimuli (e.g. mirror reading) are associated more with dorsal stream activity and the cerebellum [13], so it may be the case that in normal subjects the role of the ventral stream (with the fusiform gyrus one of its important elements) is simply masked, or more effectively controlled, by the more dominant activity in the dorsal part. In dyslexics the magnocellular deficit affects more the dorsal parietal areas [14]. As a result the top down inhibition from the parietal areas to the ventral areas is weakened and thus the percept generated by the activation of the ventral stream areas we have identified in this work persists a little more. This can be interpreted either as a "sluggish attentional shift" or as a prolongation of the "cognitive integration window" [15], providing an explanation of the differences in perception and the difficulties encountered by dyslexics. Dyslexic can see visual patterns in music because the persistence of the percept is long enough to break through to consciousness as a visual image [12]. Dyslexics however will have difficulties with rapid sequences of stimuli when the persistence of the percept of one stimulus interferes with the next, leading to the well-known deficits of dyslexics in processing linguistic material.

IV. Conclusion and Outlook

Our results highlight the limitations of studies using highly artificial stimuli in one sensory modality. Concepts derived from experiments using only such stimuli may reflect more the limited exploration allowed by these stimuli rather than the true nature of brain function. There is a general need for experimental designs with ecological stimuli and robust and powerful ways of analyzing the resulting data, like the ones we used here. There is also a more pressing need for methods to monitor brain function in cases where subjects cannot report what they perceived. An important example is the monitoring of brain function of infants and young children. Infants and young children cannot follow detailed instructions, they cannot control their movements and they cannot direct their attention for a long time to ecologically irrelevant simple stimuli; they do nevertheless respond well to natural stimuli in their environment, including human voice and music. The methodology proposed in this article has the potential to monitor brain activity when brain function falters and fails to extract the meaning from visual or auditory cues. The combination of these two capabilities may provide powerful new tools for identifying problems like developmental dyslexia in infancy or early childhood. The successful development of such tools will provide the opportunity for intervention much earlier when special training can be most effective.

REFERENCES

[1] J. Feldman, "Ecological expected utility and the mythical neural code," *Cogn. Neurodyn.*, vol. 4, pp. 25–35, 2010.

[2] A.A. Ioannides, "Magnetoencephalography as a research tool in neuroscience: State of the art," *The Neuroscientist*, vol. 12, pp 524-544, 2006.

[3] A.A. Ioannides, M. Popescu, A. Otsuka, A. Bezerianos, L. Liu, "Magnetoencephalographic evidence of the interhemispheric asymmetry in echoic memory lifetime and its dependence on handedness and gender," *Neuroimage*, vol. 19, pp. 161–175, 2003.

[4] M. Popescu, A. Otsuka and A.A. Ioannides, "Dynamics of brain activity in motor and frontal cortical areas during music listening: a magnetoencephalographic study," *Neuroimage*, vol. 21, pp. 1622–1638, 2004.

[5] J. Foote and S. Uchihashi "The beat spectrum: A new approach to rhythm analysis," in *IEEE International Conference on Multimedia & Expo*, 2001.

[6] A.A. Ioannides, "Real Time Human Brain Function: Observations and Inferences from Single Trial Analysis of Magnetoencephalographic Signals" Clinical EEG vol. 32, pp. 98-111, 2001.

[7] A.A. Ioannides, J.P.R.Bolton, and C.J.S. Clarke, "Continuous probabilistic solutions to the biomagnetic inverse problem," *Inverse Problems* vol. 6, pp. 523-542, 1990.

[8] J.G. Taylor, A.A. Ioannides, and H.W. Mueller-Gaertner, "Mathematical analysis of lead field expansions," *IEEE transactions on medical imaging* vol. 18, pp. 151-163, 1999.

[9] J. Talairach and P. Tournoux, *Co-planar stereotaxic atlas of the human brain*. New York: Thieme Medical Publishers, 1988.

[10] A.A. Ioannides, "Ανάλυση εικόνας και μουσικής από τον εγκέφαλο: Διαφορετικά ερεθίσματα – Όμοιοι μηχανισμοί" In: "Κατανοώντας τον ανθρώπινο εγκέφαλο" (Εθνικό Ίδρυμα Ερευνών), Athens 2009, pp. 59-82.

A.A. Ioannides, "Analysis of image and music in the brain: different stimuli – similar mechanisms". In "Understanding the human brain" (National Institute of Research), Athens 2009, pp. 59-82.

[11] K. Overy, "Dyslexia and Music: From timing deficits to musical intervention," *Ann. N.Y. Acad. Sci.*, vol. 999, pp. 497-505, 2003.

[12] G. Backhouse, "Dyslexia in a professional musician," in *Music and Dyslexia: Cambridge Conference Proceedings. Reading: British Dyslexia Association*, T.R. Miles and J. Augur, Eds., pp. 24-37, 1994.

[13] R.A. Poldrack, J.E. Desmond, G.H. Glover and J.D.E. Gabrieli, "The Neural Basis of Visual Skill Learning: An fMRI Study of Mirror Reading", *Cerebral Cortex*, vol. 8, pp. 1-10, 1999.

[14] J. Stein, "The Magnocellular Theory of Developmental Dyslexia", *Dyslexia*, vol. 7, pp. 12-36, 2001.

[15] R. Hari and H. Renvall, "Impaired processing of rapid stimulus sequences in dyslexia" Trends in Cognitive Sciences, vol. 5, pp. 525-532, 2001.